



Evolution of the residual stress in solid oxide fuel cell during creep

Xiang Zhao¹ · Yongjun Lu¹ · Xu Song¹ · Fenghui Wang¹

Received: 25 April 2018 / Accepted: 23 October 2018 / Published online: 28 October 2018
© Australian Ceramic Society 2018

Abstract

The evolutions of stress in the multilayer structure of solid oxide fuel cell (SOFC) working under high temperature are calculated by an analytical model. A finite element model is established to validate the results of the present model. The results show that, the present model can be used to analyze the stress relaxation of the SOFC during creep, the stresses both in anode and electrolyte drop dramatically at the first time, but the stress in cathode is first increased and then decreased. The stress relaxation rates of the anode, electrolyte, and cathode of SOFC are 97.87%, 94.91%, and 57.36%, respectively. The creep behavior of electrolyte has little effect on the stress redistribution of the single cell, while anode as well as cathode plays an important role in the evolution of the residual stress and curvature.

Keywords Multilayer structure · Creep deformation · Stress · Solid oxide fuel cell · Curvature

Introduction

Structural reliability, which may greatly affect the generating electricity and endurance life of solid oxide fuel cells (SOFC), has significantly impeded the commercial applications of SOFC. The issues of electrochemical performance degradation of SOFC have been exposed due to the irreversible creep deformations that existed in the SOFC system [1, 2]. The creep deformations that changed the initial mechanical and electrochemical equilibrium could lead to a local electrochemical failure, contact resistance (CR) increasing, and the leakage of gasses [3, 4].

The deformation in a cell embedded in a stack originate from the sintering phase of the manufacturing process, the joining with the components of the single repeating units frame by sealing material, and the reduction of the nickel

oxide in the anode [5, 6]. In addition, given that SOFCs are operated at high temperature, creep relieve stresses will bring a local and non-uniform irreversible deformation to a single cell and its connected component. Performance degradation or even failure will happen in the single cell when the creep deformation was accumulated [7], it is important to determine the creep parameters for studying the failure mechanism of SOFC. The data available compiled from the literature on the mechanical properties of SOFCs can meet the most stringent needs in mechanical characterizations [6], while the use of time or temperature-independent values may induce misleading predictions of the stress state. For instance, stress relief, the calculated result by finite element method (FEM) considering creep, will occur over SOFC operating time-scales. The sealing area that relies on compression of the cells will tend to relax over time [8]. A finite element simulation on a bonded compliant seal structure of a planar SOFC was performed using a creep-damage model, the results showed that reasonably reducing the thickness of filler metal and foil can decrease the damage of the bonded compliant seal structure [9], the residual stress in the cell and the bonded compliant seal can be decreased by making use of the short-time creep relaxation effect [2]. However, the thickness reduction will lead to an increase of the risk of failures of the cell due to thermal buckling, loss of gas tightness or electrical contact [10]. No detailed analysis has been performed on the influence of creep on the stress evolution process of a single cell in planar SOFC stack.

✉ Xiang Zhao
xzhao@nwpu.edu.cn

Yongjun Lu
404031503@qq.com

Xu Song
872282205@qq.com

Fenghui Wang
280154565@qq.com

¹ Department of Engineering Mechanics, Northwestern Polytechnical University, Xi'an 710129, China

The single cell of planar SOFC is a multilayer structure consisting of anode, electrolyte, and cathode. Most analyses of the stress in multilayer structure are based on linear elastic analysis. While the creep deformation in the single cell can result in stress relaxation and redistribution in the film/substrate system, very few investigations had been made for the creep analysis of layered structures. An analytical model was developed by Shen and Suresh [11] for steady-state creep deformations in multilayered materials during thermal cycling. The residual stresses, stress relaxation, and curvature during the monotonic temperature change can be predicted by this method, although the deviation of the method has not been explained clearly. An analytical model having closed-form solutions was developed by Zhang et al. [12] to estimate the effect of creep deformation on the stress relaxation and redistributions in the film/substrate bilayer system. Chen et al. [13] presented a model to elucidate either the film or the substrate subjected to creeping deformation. The results obtained by Chen's model are consistent with the simulated results, Zhang's creep solution [12] and Hsueh's viscoelastic solution [14]. However, the creep both in substrate and film should be mentioned together in many cases.

In this paper, considering the creep behaviors of substrate and film synthetically, a model that is more convenient for SOFC is proposed to predict the evolutions of stresses and deformations. It is discussed that how the creep behaviors of anode, electrolyte, and cathode affect the stress and deformation evolution of YSZ with time increasing. A FEM is set up to verify the model.

Analytical model for creep analysis

The relation between strain and curvature of a multilayer structure

In the present analysis, a single anode-supported SOFC is modeled as an elastic multilayer thin-plate in which each individual component is assumed to be an isotropic and elastic material. As schematically shown in Fig. 1, for the multilayer structure, the thickness and top surface of layer i is t_i and h_i ($i = 1, 2, \dots, n$), respectively. The corresponding thermoelastic properties are E_i , ν_i , α_i , where E is the Young's modulus, ν is the Poisson's ratio, and α is thermal expansion coefficient, respectively. Generally, layer 1 can be taken as a substrate, all other layers are films bonded to the layer 1. The coordinate axis x is located at the free surface of layer 1, and the axis y is aligned along the thickness direction of the plate pointing from the bottom surface to the top surface. Thus, the free surface of the uppermost film layer is located at $y = h_n$. According to the Bernoulli-Euler assumption [13] that planar sections perpendicular to the axis remain planar

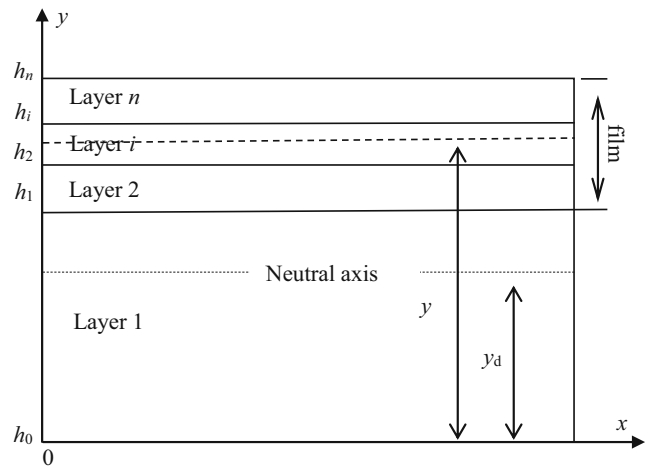


Fig. 1 Schematic of the multilayer structure and the coordinate system

after deformation due to the temperature fluctuation, the normal strain at the location y is

$$\varepsilon(y, t) = [(\rho - y_d + y)d\theta - \rho d\theta] / \rho d\theta \quad (1)$$

where y_d is the distance from the neutral axis for zero normal strain to the coordinate axis x , and ρ is the curvature radius of the neutral axis, $d\theta$ is the relative rotation angle of the two adjacent cross sections. Likewise, the normal strain at the coordinate axis x (i.e., $y = 0$) is

$$\varepsilon_0(t) = [(\rho - y_d)d\theta - \rho d\theta] / \rho d\theta \quad (2)$$

Substituting Eq. (2) into Eq. (1), the total strain in the multilayer system can be expressed as

$$\varepsilon(y, t) = \varepsilon_0(t) + k(t)y \quad (0 \leq y \leq h_n) \quad (3)$$

where $k(t) = 1/\rho$ is the curvature of the neutral axis. It should be noted that the time-dependent deformation of the system is considered due to the introduction of creep deformation in the following section. Consequently, $\varepsilon_0(0)$ and $k(0)$ denote the initial reference strain at the bottom surface of the substrate and initial curvature, respectively.

Creep deformation in the multilayer structure

When creep deformation is considered in the system, based on the generalized Hooke's law, the constitutive relationship taking into account the thermal mismatch and creep deformation, simultaneously, can be expressed as

$$\sigma_i(y, t) = E_i^* [\varepsilon_i(y, t) - \alpha_i \Delta T - \varepsilon_i^{cr}(y, t)] \quad (i = 1, 2, \dots, n) \quad (4)$$

where E_i^* is the biaxial modulus defined as $E_i^* = E_i / (1 - \nu_i)$, ΔT is the change of temperature, and ε_i^{cr} is the accumulated creep strain in layer i . For primary and the stationary creep regime,

the inelastic stress-creep strain of the individual layer is governed by the classical power law model

$$\dot{\varepsilon}_i^{cr} = A\sigma_i^n \tag{5}$$

in which the superscript dot denotes the derivative with respect to time t , A is the creep constant, and n is the stress exponent.

Without the action of external loading, the equilibrium equations for the axial force and bending moment of the multilayer system are given as

$$\sum_{i=1}^n \int_{h_{i-1}}^{h_i} \sigma_i(\varsigma, t) d\varsigma = 0 \tag{6}$$

$$\sum_{i=1}^n \int_{h_{i-1}}^{h_i} \sigma_i(\varsigma, t) \varsigma d\varsigma = 0 \tag{7}$$

It needs to point out that when $i = 1$, h_{i-1} (i.e. h_0) is defined as zero. When $t = 0$, the creep strain is absent, by substituting Eqs. (3) and (4) into Eqs. (6) and (7), one can yield

$$\varepsilon_0(0)C_1 + k(0)C_2 = N \tag{8}$$

$$\varepsilon_0(0)C_2 + k(0)C_3 = M \tag{9}$$

in which

$$C_1 = \sum_{i=1}^n E_i t_i \quad C_2 = \frac{1}{2} \sum_{i=1}^n E_i (h_i^2 - h_{i-1}^2)$$

$$N = \sum_{i=1}^n E_i \alpha_i \Delta T t_i \quad C_3 = \frac{1}{3} \sum_{i=1}^n E_i (h_i^3 - h_{i-1}^3)$$

$$M = \frac{1}{2} \sum_{i=1}^n E_i \alpha_i \Delta T (h_i^2 - h_{i-1}^2)$$

Thus, $\varepsilon_0(0)$ and $k(0)$ can be by obtained by Eqs. (8) and (9)

$$\varepsilon_0(0) = (C_2 M - C_3 N) / (C_2^2 - C_1 C_3) \tag{10}$$

$$k(0) = (C_2 N - C_1 M) / (C_2^2 - C_1 C_3) \tag{11}$$

Then, the initial thermoelastic stresses responsible for ensuing creep response in layer i can be calculated from

$$\sigma_i(y, 0) = E_i^* [\varepsilon_0(0) + k(0)y - \alpha_i \Delta T] \quad (i = 1, 2, \dots, n) \tag{12}$$

When $t > 0$, the creep deformation occurs within the system. By differentiating Eqs. (6) and (7) with respect to t , along with

some algebraic manipulation, the reference strain rate $\dot{\varepsilon}_0(t)$ and curvature change rate $k(t)$ can be obtained by

$$\dot{\varepsilon}_0(t) = (C_2 Q - C_3 P) / (C_2^2 - C_1 C_3) \tag{13}$$

$$\dot{k}(t) = (C_2 P - C_1 Q) / (C_2^2 - C_1 C_3) \tag{14}$$

in which

$$P = \sum_{i=1}^n \int_{h_{i-1}}^{h_i} E_i^* \dot{\varepsilon}_i^{cr}(y, t) dy$$

$$Q = \sum_{i=1}^n \int_{h_{i-1}}^{h_i} E_i^* \dot{\varepsilon}_i^{cr}(y, t) y dy$$

Again, making use of Eqs. (3) and (4), and carrying out the derivative with respect to time, the total strain rate and the stress rate in the system can be written as

$$\dot{\varepsilon}(y, t) = \dot{\varepsilon}_0(t) + k(t)y \tag{15}$$

$$\dot{\sigma}_i(y, t) = E_i^* [\dot{\varepsilon}_0(t) + k(t)y - \dot{\varepsilon}_i^{cr}] \tag{16}$$

It is evident that a combination of Eqs. (5), (14), (15), and (16) gives the partial differential governing equations for the development of stress and deformation with time in the system. Once the initial condition (i.e., Eq. (12)) is prescribed, the finite difference method is validated to be efficient for solving governing equations incrementally. For example, at any given time, the stress evolve with a time step can be calculated by

$$\sigma_i(y, t + \Delta t) = \sigma_i(y, t) + \dot{\sigma}_i(y, t) \Delta t \tag{17}$$

In this paper, all the iterative steps are implemented using Comsol Multiphysics.

Model geometry of the single cell of SOFC

The single cell of planar SOFC is a triple-layer structure consisting of anode, electrolyte, and cathode. Figure 2 illustrates the fabrication process of Ni-YSZ/YSZ/LSM single cells. First, the resultant NiO/YSZ powders were uniaxially pressed as a green substrate. Proper amount of YSZ powders and the substrate were then co-pressed to form a green bilayer and subsequently co-fired at 1400 °C in air for 4 h to densify the YSZ film. Cathode was prepared on the electrolyte with a screen-printing technique using slurry made of La_{0.5}Sr_{0.4}MnO₃ (LSM). Single cells were achieved after

Fig. 2 Schematic protocol for preparing infiltrated electrodes

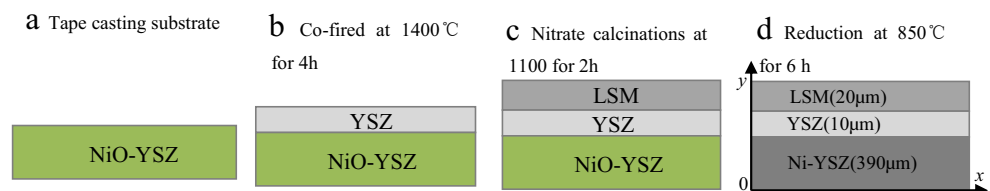


Table 1 Material properties of SOFC materials

	Temp	Anode Ni-YSZ	Electrolyte YSZ	Cathode LSM
E (GPa)	293 K	67[15]	224[15]	41[16]
	1073	53[15]	144[16]	52[16]
	1273 K	49[15]	157[16]	53[16]
ν	298 K	0.39[3]	0.29[17]	0.28[3]
	1073 K	0.39[3]	0.29[17]	0.28[3]
$\alpha(\times 10^{-6})$	350 K	9.48[18]	9.93[17]	11.51[19]
	1073 K	12.41[18]	10.35[20]	12.19[19]
	1273 K	12.74[20]	10.30[20]	12.63[19]
A	1073 K	2.60×10^{-11}	1.18×10^{-14}	1.27×10^{-12}
		n	1.7[2]	1[1]

calcinations at 1100°C for 2 h. Finally, NiO in anode have to be reduced to Ni at 850 °C in hydrogen.

Finite element model of the single cell of SOFC

An axisymmetric finite element model (FEM) was generated by the commercial code Abaqus following the geometry shown in Fig. 2d. The thickness of Ni-YSZ, YSZ, and LSM are 390 μm , 10 μm , and 20 μm , respectively. The length of the cell is 8.4 mm (4.2 mm in the axisymmetric model). The symmetric axis is located at the left side of the cell. The left node on the bottom face was fixed to make sure there is no large displacement during the simulation. Using the CAX4R bilinear axisymmetric quadrilateral element from the Abaqus element library, the solution was demonstrated to be mesh independent when the number of the elements is greater than 104,000.

Results and discussion

The available thermoelastic material properties in the literature for solid, fully dense material samples relevant to SOFCs, are summarized in Table 1 as a function of temperature. Where there is a variation of material properties such as E with temperature a linear interpolation is assumed between the data points quoted from the literature.

At high temperature, thermal stresses generate because of the mismatch CTE between layers of SOFC. Previous study indicates that stresses are relieved by plastic flow for temperature above 1200 °C [22]. Considering the behavior of plastic flow under high temperature, the fictitious zero-stress temperature for the half-cell composed of anode and electrolyte is supposed to be 1200 °C in the present study [22, 23]. When the half-cell is cooled to operation temperature of 800 °C from

zero-stress temperature, both the cooling temperature difference ΔT_1 and ΔT_2 are -400 °C. While ΔT_3 for cathode is 300 °C due to the calcinations temperature is 1100 °C. After the initial thermal stress at 800 °C is calculated, the creep analysis of 10,000 h is carried out in the following step.

The evolutions of stress and strain in the single cell can be calculated by the analytical model and FEM described in “Analytical model for creep analysis” and “Finite element model of the single cell of SOFC” sections, respectively. Here we define the stress along X-direction as the axial stress (σ_1). Correspondingly, the creep strains are defined as axial strain (ε_1), if the effect of clamping load (a single cell in an SOFC stack have to endure a clamping load) on the stress and deformation is not taken into account.

Initial residual stress in the single cell

Assuming that there is no creep deformation occurred in the cell until anode (NiO-YSZ) has been reduced. That is, only elastic deformation occurred during the process of sintering, calcinations, and reduction. The initial residual stress in three layers is shown in Fig. 3. It can be seen that the results calculated by the proposed model are in excellent agreement with finite element simulation. The anode substrate undergoes a stress transition from -6.38 MPa (for $y=0$) to 13.06 MPa (for $y=0.390$ mm) along the thickness direction. The initial zero stress axis of the cell is located at $y=0.126$ mm. The stress in electrolyte film (YSZ) ranges from -136.49 to -135.43 MPa. In cathode film (LSM), the stress is changed from 4.97 to 5.77 MPa.

Creep stress and deformation in the single cell

The initial equilibrium state, residual stress, and deformation, will change due to anode, electrolyte, and cathode tending to creep when they are subjected to stress at high temperatures. The variation of the stress and deformation in electrodes can be calculated according to the foregoing proposed model.

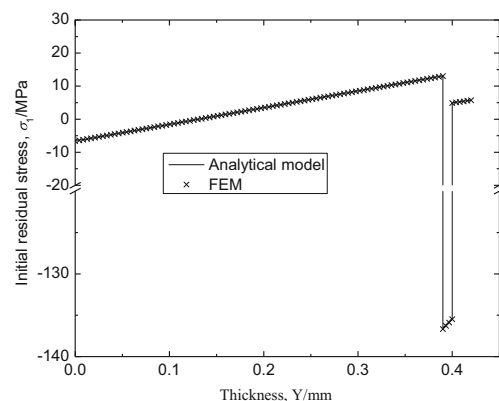


Fig. 3 Residual stress in Ni-YSZ, YSZ, and LSM along Y direction

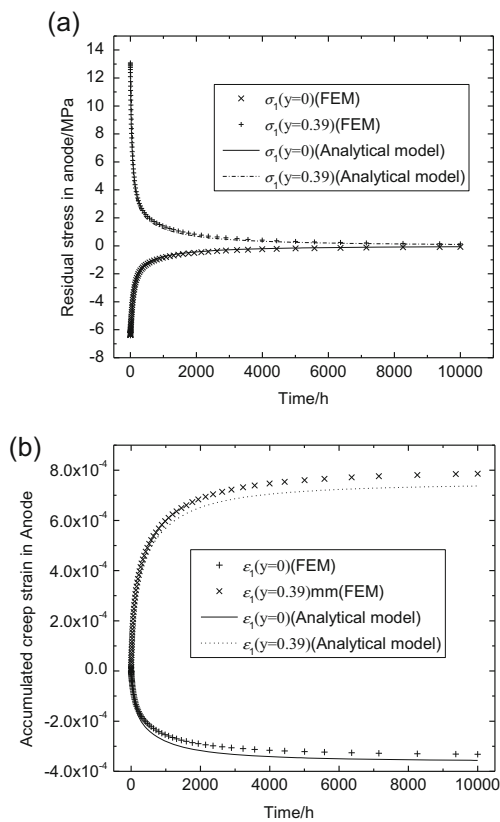


Fig. 4 The evolutions of **a** stress and **b** accumulated creep strain in anode at the free surface ($y = 0$) and that near the anode/electrolyte interface ($y = 0.39$ mm)

Anode

Figure 4a shows the evolution of stress in anode. For the legends in Fig. 4a, the $\sigma_1(y = 0)$ and $\sigma_1(y = 0.39)$ denote the equal bi-axial stress in the free surface of anode located at $y = 0$, and the surface of anode at the anode/electrolyte interface located at $y = 0.39$ mm, respectively. It can be seen that both of the stresses drop dramatically at the first time but decrease slowly with the time increasing. The stress in the free surface of anode decreases from -6.38 MPa in the elastic step to -0.16 MPa at $t = 10,000$ h during creep. Correspondingly, the change of stress in anode near the anode/electrolyte interface is from 13.06 to 0.28 MPa.

The evolutions of the accumulated creep strains with time in anode are given in Fig. 4b. Generally, a high stress will lead to a large creep strain rate according to Eq. (5). With the time increasing, the accumulated creep strain in anode increases dramatically and thus leads to the suddenly decreased stress.

Electrolyte and cathode

The evolution of stress in electrolyte is shown in Fig. 5. For electrolyte, the initial stress (at the center of the electrolyte) is -135.96 MPa, while -6.92 MPa after creep of $10,000$ h. The

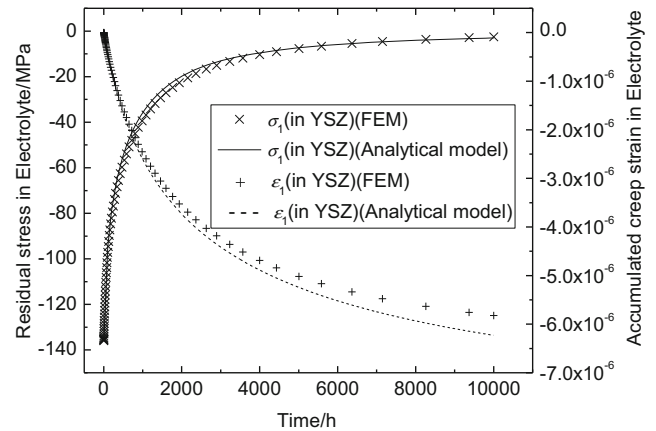


Fig. 5 The stress and accumulated creep strain in electrolyte

stress relaxation rate of electrolyte can be obtained as 94.91% . In comparison, the evolution of the stress in cathode is remarkably different from that in anode and electrolyte, as shown in Fig. 6. In the one hand, the stress relaxation rate is only 57.36% compared with that of anode and electrolyte. On the other hand, the stress starts at the initial stress, increases quickly to a peak value (19.25 MPa at 424 h), and then decrease gradually to a minimum (2.29 MPa at $10,000$ h). This unexpected overshoot behavior in cathode during creep process in contrast to the case of anode and electrolyte can be attributed to the creep rate mismatch [24] between anode and cathode. In other word, as the anode dominates creep deformation of overall cell (shown in the next section), the cathode is forced to tension, resulting in an increase in stress for maintaining the displacement continuity. When the creep rate induced by stress in cathode is fast enough to pursue the overall deformation, sequentially, the onset of stress drooping in cathode can be observed. In this sense, the overshoot behavior of stress in cathode can be regarded as the creep resistance during initial stage of creep.

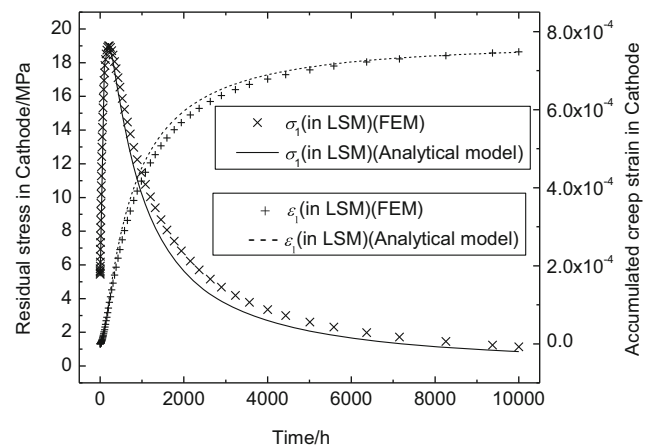


Fig. 6 The stress and accumulated creep strain in cathode

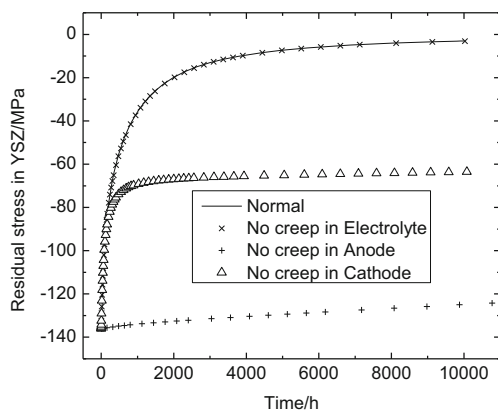


Fig. 7 Comparison of the stresses in electrolyte in different situations

The effect of the creep behaviors of electrodes on the stress evolution

After closer inspection in regard to those accumulated creep strains obtained above, we find that the creep deformation of electrolyte (-6.23×10^{-6} at 10000 h) is so small that it can be ignored. Consequently, the problem arising from the inspection is that which layer may play significant effect on the stress evolution of a single cell during creep. Therefore, three different situations that the absence of creep deformation in NiO-YSZ, YSZ and LSM are investigated, respectively.

The stresses in electrolyte YSZ for different cases calculated by the analytical model and FEM are shown in Fig. 7. Upon neglecting creep contribution from different component, one can observe various stress relaxation behavior. When the creep behavior of anode is not considered, the stress in YSZ displays the least stress shift relative to the initial stress at the operating temperature of 800 °C. Therefore, one can conclude that the creep contribution of anode plays the most important role in the evolution of stress in the triple-layer structure. While the creep deformation of cathode is neglected, as shown in Fig. 7, the moderate stress relaxation rate of about 51.15% can be obtained after 10,000 h, reflecting the secondary importance of creep deformation in cathode for the structure stress relaxation. In contrast, the creep behavior of electrolyte can be ignored, because it brought little change of the stress evolution compared with the normal case that the creep behavior of all the components are regarded.

The role of creep contribution for respective layer can also confirmed by the changes of the curvature of the single cell. The effects of creep behavior for anode, electrolyte, and cathode, respectively, are reproduced from Fig. 8, which is similar with that of the residual stresses in Fig. 7. It can be seen that the curvatures are increased with time and both the creep behaviors of anode and cathode cannot be ignored.

It should be noted that, although these obtained results are based on the particular geometry in terms of anode-supported SOFC, the methodology and the model incorporating creep deformation for multilayer system presented in this paper are

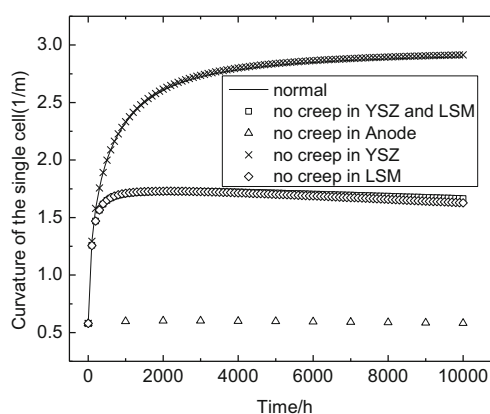


Fig. 8 Comparison of the curvatures of the single cell in different situations

general. In principle, the creep deformation and stress relaxation within a multilayered system are dependent on the thickness of individual layer and corresponding material parameter related to it, according to Eqs. (13) and (14). That is to say, it is possibility to study other types of planar SOFC, such as cathode-supported scenario, as long as we know the corresponding input parameter including the structure parameters and creep properties. In addition, during reduction process, several complicated chemical strain [25], plastic deformation [26], and novel accelerated creep [27] were introduced, which can actually modify the initial stresses, hence ensuing creep responds, whereas are not considered in our model. Given that SOFC is operated at high temperature, creep and stress relaxation of the multilayer structure will impact the contact resistance of SOFC [28], a more sophisticated model incorporating this phenomenon during reduction may be considered for further study for precise prediction of the creep responds.

Conclusions

The single cell of SOFC is a triple-layer structure operating at high temperature. The creep behaviors of anode, electrolyte, and cathode can result in a stress relaxation and redistribution, and then bring a local and non-uniform irreversible deformation to the single cell and its connected component. In this study, an analytical model was presented to study the stress evolution of the SOFC. The results obtained by this method are in agreement with that calculated by FEM. The stresses both in anode and electrolyte will drop dramatically at the first time but decrease slowly with the time increasing. While the stress in cathode is first increased and then decreased. The evolution of stress in the single cell is greatly affected by the creep behavior of anode and cathode but little by electrolyte.

Funding information This work was supported by the National Natural Science Foundation of China (11572253) and the Fundamental Research Funds for the Central Universities (3102014JCQ01040).

References

- Greco, F., Frandsen, H.L., Nakajo, A., Madsen, M.F., Herle, J.V.: Modelling the impact of creep on the probability of failure of a solid oxide fuel cell stack. *J Eur Ceram Soc.* **34**, 2695–2704 (2014)
- Laurencin, J., Delette, G., Usseglio-Viretta, F., Iorio, S.D.: Creep behaviour of porous SOFC electrodes: measurement and application to Ni-8YSZ cermets. *J Eur Ceram Soc.* **31**, 1741–1752 (2011)
- Nakajo, A., Mueller, F., Brouwer, J., Herle, J.V., Favrat, D.: Mechanical reliability and durability of SOFC stacks. Part II: modelling of mechanical failures during ageing and cycling. *Int J Hydrog Energy.* **37**, 9269–9286 (2012)
- Zhang, Y.C., Zhao, H.Q., Jiang, W.C., Tu, S.T., Zhang, X.C., Wang, R.Z.: Time dependent failure probability estimation of the solid oxide fuel cell by a creep-damage related Weibull distribution model. *Int J Hydrog Energy.* **43**, 13532–13542 (2018)
- Kurama, S., Saydam, G.: Investigation properties of BaO/RO - Al₂O₃ -R₂O₃ -B₂O₃ - SiO₂ glass-ceramic sealants for solid oxide fuel cell. *J Aust Ceram Soc.* **53**, 293–298 (2017)
- Nakajo, A., Kuebler, J., Faes, A., Vogt, U.F., Schindler, H.J., Chiang, L.K., Modena, S., Herle, J.V., Hocker, T.: Compilation of mechanical properties for the structural analysis of solid oxide fuel cell stacks. Constitutive materials of anode-supported cells. *Ceram Int.* **38**, 3907–3927 (2012)
- Jiang, W.C., Luo, Y., Zhang, W.Y., Woo, W.C., Tu, S.T.: Effect of temperature fluctuation on creep and failure probability for planar solid oxide fuel cell. *J Fuel Cell Sci Technol.* **12**, 051004 (2015)
- Clague, R., Marquis, A.J., Brandon, N.P.: Finite element and analytical stress analysis of a solid oxide fuel cell. *J Power Sources.* **210**, 224–232 (2012)
- Zhang, Y.C., Jiang, W., Tu, S.T., Wen, J.F.: Simulation of creep and damage in the bonded compliant seal of planar solid oxide fuel cell. *Int J Hydrog Energy.* **39**, 17941–17951 (2014)
- Nakajo, A., Wuillemin, Z., Jan, V.H., Favrat, D.: Simulation of thermal stresses in anode-supported solid oxide fuel cell stacks. Part II: loss of gas-tightness, electrical contact and thermal buckling. *J Power Sources.* **193**, 216–226 (2009)
- Shen, Y.L., Suresh, S.: Steady-state creep of metal-ceramic multilayered materials. *Acta Mater.* **44**, 1337–1348 (1996)
- Zhang, X.C., Xu, B.S., Wang, H.D., Wu, Y.X.: Residual stress relaxation in the film/substrate system due to creep deformation. *J Appl Phys.* **101**, 083530 (2007)
- Chen, Q.Q., Xuan, F.Z., Tu, S.T.: Modeling of creep deformation and its effect on stress distribution in multilayer systems under residual stress and external bending. *Thin Solid Films.* **517**, 2924–2929 (2009)
- Hsueh, C.H.: Modeling of elastic deformation of multilayers due to residual stresses and external bending. *J Appl Phys.* **91**, 9652–9656 (2002)
- Pihlatie, M., Kaiser, A., Mogensen, M.: Mechanical properties of NiO/Ni-YSZ composites depending on temperature, porosity and redox cycling. *J Eur Ceram Soc.* **29**, 1657–1664 (2009)
- Giraud, S., Canel, J.: Young's modulus of some SOFCs materials as a function of temperature. *J Eur Ceram Soc.* **28**, 77–83 (2008)
- Pratihari, S., Dassharma, A., Maiti, H.: Properties of Ni/YSZ porous cermets prepared by electroless coating technique for SOFC anode application. *J Mater Sci.* **42**, 7220–7226 (2007)
- Meinhardt, K.D., Kim, D.S., Chou, Y.S., Weil, K.S.: Synthesis and properties of a barium aluminosilicate solid oxide fuel cell glass-ceramic sealant. *J Power Sources.* **182**, 188–196 (2008)
- Mori, M., Hiei, Y., Sammes, N.M., Tompsett, G.A.: Thermal-expansion behaviors and mechanisms for Ca- or Sr-doped lanthanum manganite perovskites under oxidizing atmospheres. *J Electrochem Soc.* **147**, 1295–1302 (2000)
- Skarmoutsos, D., Tsoga, A., Naoumidis, A., Nikolopoulos, P.: Solid oxide fuel cells. *Solid State Ionics.* **135**, 439–444 (2000)
- Lipińska-Chwałek, M., Pećanac, G., Malzbender, J.: Creep behaviour of membrane and substrate materials for oxygen separation units. *J Eur Ceram Soc.* **33**, 1841–1848 (2013)
- Atkinson, A., Selçuk, A.: Residual stress and fracture of laminated ceramic membranes. *Acta Mater.* **47**, 867–874 (1999)
- Lu, Y.J., Zhang, K., Wang, F.H., Lou, K., Zhao, X.: Enhanced and weakened strength in brittle film-substrate structure. *Mater Des.* **108**, 455–461 (2016)
- Limarga, A.M., Wilkinson, D.S.: Modeling the interaction between creep deformation and scale growth process. *Acta Mater.* **55**, 189–201 (2007)
- Sarantaridis, D., Chater, R.J., Atkinson, A.: Changes in physical and mechanical properties of SOFC Ni-YSZ composites caused by redox cycling. *J Electrochem Soc.* **155**, 467–472 (2008)
- Sun, B., Rudkin, R.A., Atkinson, A.: Effect of thermal cycling on residual stress and curvature of anode-supported SOFCs. *Fuel Cells.* **9**, 805–813 (2009)
- Frandsen, H.L., Makowska, M., Greco, F., Chatzichristodoulou, C., Ni, D.W., Curran, D.J., Strobl, M., Kuhn, L.T., Hendriksen, P.V.: Accelerated creep in solid oxide fuel cell anode supports during reduction. *J Power Sources.* **323**, 78–89 (2016)
- Comminges, C., Fu, Q.X., Zahid, M., Steiner, N.Y., Bucheli, O.: Monitoring the degradation of a solid oxide fuel cell stack during 10,000 h via electrochemical impedance spectroscopy. *Electrochim Acta.* **59**, 367–375 (2012)